Biosensors and Bioelectronics 36 (2012) 161–167

Contents lists available at SciVerse ScienceDirect

Biosensors and Bioelectronics

journal homepage: www.elsevier.com/locate/bios

# Gold-nanobeacons for real-time monitoring of RNA synthesis

João Rosa [a,b,1], João Conde [a,c,1], Jesus M. de la Fuente [c], João C. Lima [b], Pedro V. Baptista [a,*]

[a] CIGMH, Departamento de Ciências da Vida, Faculdade de Ciências e Tecnologia, Universidade Nova de Lisboa, Campus de Caparica, 2829-516 Caparica, Portugal
[b] REQUIMTE, Departamento de Química, Faculdade de Ciências e Tecnologia, Universidade Nova de Lisboa, Campus de Caparica, 2829-516 Caparica, Portugal
[c] Instituto de Nanociencia de Aragón, Universidad de Zaragoza, Campus Ri˙o Ebro, Edifi˙cio I+D, Mariano Esquillor, s/n, 50018 Zaragoza, Spain

ARTICLE INFO

*Article history:*
Received 31 January 2012
Received in revised form
20 March 2012
Accepted 9 April 2012
Available online 20 April 2012

*Keywords:*
Gold nanoparticles
Fluorophore labeled hairpin-DNA
Gold-nanobecons
RNA synthesis
Inhibition of transcription

ABSTRACT

Measuring RNA synthesis and, when required, the level of inhibition, is crucial towards the development of practical strategies to evaluate silencing efficiency of gene silencing approaches. We developed a direct method to follow RNA synthesis in real time based on gold nanoparticles (AuNPs) functionalized with a fluorophore labeled hairpin-DNA, *i.e.* gold-nanobeacon (Au-nanobeacon). Under hairpin configuration, proximity to gold nanoparticles leads to fluorescence quenching; hybridization to a complementary target restores fluorescence emission due to the Au-nanobeacons' conformational reorganization that causes the fluorophore and the AuNP to part from each other, yielding a quantitative response. With this *reporter* Au-nanobeacon we were able to measure the rate of *in vitro* RNA synthesis (~10.3 fmol of RNA per minute). Then, we designed a second Au-nanobeacon targeting the promoter sequence (*inhibitor*) so as to inhibit transcription whilst simultaneously monitor the number of promoters being silenced. Using the two Au-nanobeacons in the same reaction mixture, we are capable of quantitatively assess in real time the synthesis of RNA and the level of inhibition.

The biosensor concept can easily be extended and adapted to situations when real-time quantitative assessment of RNA synthesis and determination of the level of inhibition are required. In fact, this biosensor may assist the *in vitro* evaluation of silencing potential of a given sequence to be later used for *in vivo* gene silencing.



## 1. Introduction

Monitoring and controlling RNA synthesis is of great relevance for understanding the cell (and the organism) homeostasis. The ability to scrutinize cellular processes *in vitro* has become an important tool for novel approaches to gene studies and for molecular therapeutics (Agrawal, 1996; Fichou and Ferec, 2006; Tamm et al., 2001; Toub et al., 2006). Several techniques to analyze RNA synthesis *in vitro* have been described, *e.g.* Northern Blot (Bor et al., 2006), RT-PCR (Freeman et al., 1999; Weis et al., 1992) and cDNA microarrays (Schena et al., 1995). In addition, molecular beacons have provided a rapid and sensitive system capable of efficient quantitative monitoring of RNA synthesis and/or inhibition in real-time. A molecular beacon is a stem–loop DNA single-stranded-oligonucleotide that carries a fluorophore and a quencher at both ends: in absence of target, the stem–loop structure is closed forcing the fluorophore and the quencher to close proximity, resulting in fluorescence quenching; upon hybridization to a complementary target the stem–loop sequence opens, the fluorophore and quencher are spatially separated and the fluorescence is restored (Tan et al., 2004; Tyagi and Kramer, 1996). Fluorescence monitoring allows quantitative kinetic analysis of the conformation changes occurring in the molecular beacon under various situations such as real-time monitoring of DNA cleavage caused by enzymes (Li et al., 2000a, 2000b), protein–DNA interaction studies (Li et al., 2000a, 2000b), real-time *in vitro* transcription monitoring (Liu et al., 2002; Marras et al., 2004) and real-time PCR detection (Waltz et al., 2005).

Although robust, traditional molecular beacons can be easily degraded by nucleases that are often residually present in reaction mixtures and/or in cellular extracts, rendering the beacons ineffective. Gold nanoparticles (AuNPs) can overcome this problem by conferring protection against nucleases (Conde et al., 2010; Rosi et al., 2006) whilst maintaining the quenching and sensing properties of the beacon (Baptista et al., 2008; Baptista, 2009; Lakowicz, 2006; Paciotti et al., 2004; Quarta et al., 2007; Saha et al., 2012; Seferos et al., 2007). The combination of the optical properties of AuNPs with fluorophores in a molecular beacon conformation (Au-nanobeacon) have been used to detect sequence-specific DNA targets (Song et al., 2009) and even be more sensitive in detecting single-mismatch than regular molecular beacons (Dubertret et al., 2001).

Recently, we have assisted to a renewed interest in gene silencing strategies that aim to decrease the effective capability

* Corresponding author. Tel./fax: +351 212948530.
*E-mail address:* pmvb@fct.unl.pt (P.V. Baptista).
[1] These authors contributed equally to the work.

0956-5663/$ - see front matter © 2012 Elsevier B.V. All rights reserved.
http://dx.doi.org/10.1016/j.bios.2012.04.006

of a given gene to express itself, either by an inhibition of transcription or via an increased specific degradation. In fact, ssDNA-functionalized AuNPs have already been used in modulation of *in vitro* transcription and translation (Agbasi-Porter et al., 2006; Conde et al., 2010). Evaluation of transcription inhibition is usually assessed mainly by end-point quantification of RNA synthesis and comparison to transcription levels without silencing. However, when evaluating the effectiveness of inhibition, it is of utmost relevance to ascertain the number of molecules being *de facto* silenced, and correlating the level of inhibition to that of product production (*i.e.* RNA). Doing so in real-time would also provide information on the kinetics involved, thus yielding important information towards optimization of silencing strategy, re-design of target and effector sequences, etc (Rayburn and Zhang, 2008).

Here, we present a two-gold-nanobeacon system for the real-time monitorization of RNA transcription and inhibition: one Au-nanobeacon monitors the transcription level (*reporter*), and a second Au-nanobeacon acts as inhibitor of transcription (*inhibitor*) that quantitatively assesses the number of sequences being inhibited. Because the inhibitor reports on the number of targets it binds to, we attain real time quantification of the number of sequences being silenced at one time, and the consequent effect on transcription is provided by the reporter Au-nanobeacon—Fig. 1. This dual-biosensing system may be a practical and straightforward tool for kinetics and mechanistic studies in gene silencing approaches.

## 2. Experimental details

### 2.1. Materials

All chemicals were purchased from Sigma Aldrich in the highest purity available and used without further purification. T7 RNA Polymerase and Revert-Aid™ M-MuLV Reverse Transcriptase were purchased from Fermentas. DNase I and SYBR® GreenER Real-Time PCR Kit purchased from Invitrogen. All oligonucleotides were purchased from STAB Vida, Portugal.

### 2.2. Synthesis of citrate–gold nanoparticle

Gold nanoparticles with an average diameter of ~14 nm were synthesized by the citrate reduction method described by Lee and Meisel (1982). Briefly, 1 mM hydrogen tetrachloroaureate (III) hydrate (88.61 mg) was dissolved in 500 ml of distilled water, heated and stirred under reflux. Then, 38.8 mM sodium citrate tribasic dihydrate (285 mg) was added resulting in a red solution. The solution is kept under ebullition and protected from light for 30 min. After this, the solution is cooled down to room temperature

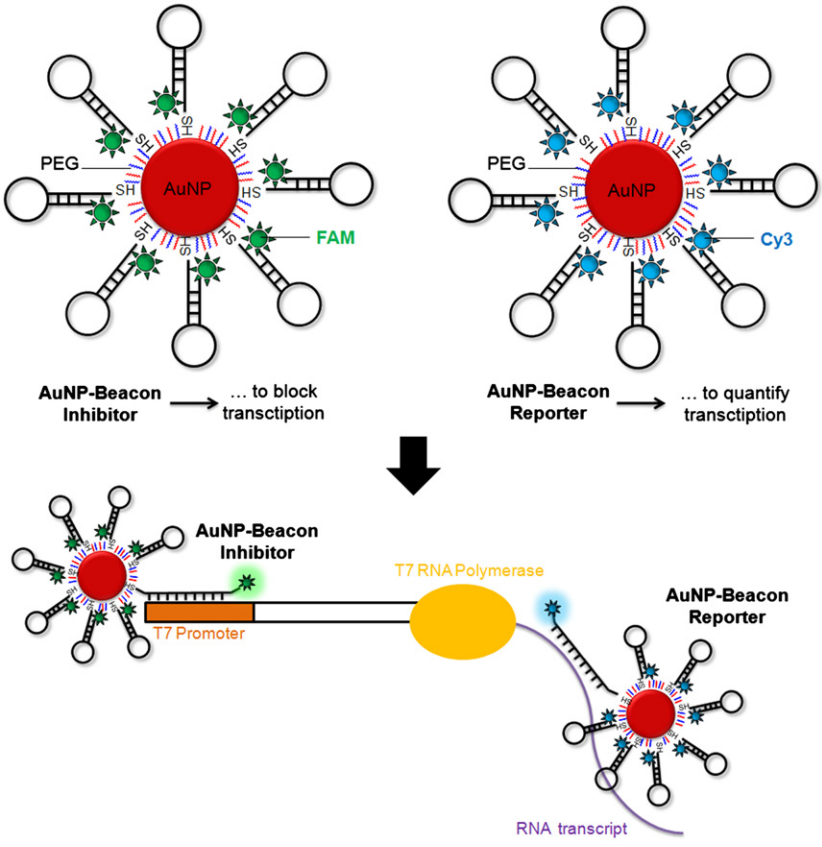


**Fig. 1.** *Gold-nanobeacons for monitoring and inhibition of real-time RNA synthesis.* An Au-nanobeacon is composed of a hairpin DNA structure with a gold nanoparticle at 5′ and a fluorophore at 3′. When the hairpin has its stem–loop structure formed, the fluorophore is forced to be in close proximity with gold nanoparticles and fluorescence is quenched due to gold nanoparticles modulation properties on standard organic fluorophores. On the other hand, in the presence of a target that can hybridize with the loop sequence of the hairpin the stem–loop structure is opened and the fluorophore is parted from the gold nanoparticles resulting in restoration of fluorescence. A cy3-labeled Au-nanobeacon hybridizes with the RNA transcript as it is formed in an *in vitro* reaction acting as a reporter of the levels of transcription. Simultaneously, a FAM-labeled Au-nanobeacon is used to hybridize with the T7 promoter region of the dsDNA template which results in inhibition of *in vitro* transcription. The fluorescence of both Au-nanobeacons is measured and quantification of both as to how many T7 promoter sites are being blocked and how many RNA products are being formed is retrieved.

and kept protected from light. Citrate–gold nanoparticles were characterized by Transmission Electron Microscopy (TEM) and UV–vis spectroscopy (see Figure S1 in Supplementary Information).

### 2.3. Gold-nanobeacons syntheses

We prepared two gold-nanobeacons: the inhibitor, a stem–looped oligonucleotide double labeled with 3′-FAM and 5′-Thiol-C6 (5′-TTTGCATCTCCCTATAGTGAGTCGTATTATGCAAA-3′) complementary to the promoter region recognized by T7-RNA polymerase, thus capable of blocking the transcriptional machinery at the specific promoter site; the reporter, a stem–looped oligonucleotide double labeled with 3′-Cy3 and 5′-Thiol-C6 (5′-TTTGCATAGCTGTTCAAGTTTGTGTTTCATGCAAA-3′) complementary to the *c-MYC* transcript produced by *in vitro* transcription—see below. Briefly, the thiolated oligonucleotides (STAB Vida, Portugal) were suspended in 1 mL of 0.1 M dithiothreitol (DTT), extracted three times with ethyl acetate and further purified through a desalting NAP-5 column (Pharmacia Biotech, Sweden) using 10 mM phosphate buffer (pH 8) as eluent. Following oligonucleotide quantification via UV/Vis spectroscopy, each oligomer was added to the AuNP solution in a 50:1 ratio. AGE I solution (2% (w/v) SDS, 10 mM phosphate buffer (pH 8)) was added to the mixture to achieve a final concentration of 10 mM phosphate buffer (pH 8), 0.01% (w/v) SDS. The solution was sonicated for 10 s using an ultrasound bath and incubated at room temperature for 20 min. After this period, 0.045 mg/mL of O-(2-Mercaptoethyl)-O′-methyl-hexa(ethylene glycol), $C_{15}H_{32}O_7S$ was added to the mixture and incubated for another 20 min at room temperature. Afterwards, the ionic strength of the solution was increased sequentially in 50 mM NaCl increments by adding the required volume of AGE II solution (1.5 M NaCl, 0.01% (w/v) SDS, 10 mM phosphate buffer (pH 8)) up to a final concentration of 10 mM phosphate buffer (pH 8), 0.3 M NaCl, 0.01% (w/v) SDS. After each increment, the solution was sonicated for 10 s and incubated at room temperature for 20 min before the next increment. Following the last addition, the solution was left to rest for additional 16 h at room temperature. Then, the functionalized Au-nanobeacons were centrifuged for 20 min at $21{,}460 \times g$, the oily precipitate washed three times with DEPC-treated $H_2O$, and redispersed in the same buffer to a final concentration in Au-nanobeacons of 15 nM. The resulting Au-nanobeacons were stored in the dark at 4 °C until further use.

### 2.4. Quantitation of beacon coverage on AuNPs

Coverage, *i.e.* average number of labeled beacons per nanoparticle was assessed following complete displacement of the thiolated oligonucleotides (beacons) from the AuNP by means of 0.12 mM β-Mercapthoethanol incubation for 48 h. After 48 h at room temperature, the solutions were centrifuged at 14500*g* for 20 min. The concentration of beacon in the supernatant was measured by monitoring the emission spectra of FAM (Exc = 490 nm) or Cy3 (Exc = 530 nm) dyes in a Cary Eclipse (Varian, USA) using an Ultra-Micro quartz cell (Hëllma, Germany). All the AuNPs samples and the standard solutions of the thiol-oligonucleotide beacon were kept at the same pH and ionic strength and calibration for all measurements. Fluorescence emission was converted to molar concentrations of the thiol modified oligonucleotide by interpolation from a standard linear calibration curve. Standard curves were prepared with known concentrations of beacon using the same buffer pH, salt, and β-Mercapthoethanol concentrations. The average number of molecular beacon strands per particle was obtained by dividing the oligonucleotide molar concentration by the AuNP concentration.

### 2.5. RNA extraction and cDNA production

Total RNA extracted from HL-60 cells was subjected to RT for cDNA synthesis with Revert-AidTM M-MuLV Reverse Transcriptase (Fermentas, Vilnius, Lithuania) according to the manufacturer's specifications, using 20 μM of MYCreverse primer, annealing at 42 °C for 1 h and 70 °C for 10 min to reverse transcriptase inactivation. Gene specific primers MYCforward: 5′-GCTCATTTCTGAAGAGGACTTGT-3′ and MYCreverse: 5 ≤ -AGGCAGTTTACATTATGGCTAAATC-3′ can then be used to PCR amplify a 229-bp fragment of the human v-myc myelocytomatosis viral oncogene homolog (c-MYC) gene (Gene-Bank accession no. NM_002467.4).

### 2.6. Transcription template preparation and purification

PCR amplification of the c-MYC specific fragment was performed in duplicate on a MyCycler Thermocycler (Biorad) in 25 μL using 1 μM of primers, 2.5 mM dNTPs with 1 U Taq DNA Polymerase (Amersham Biosciences, GE Healthcare, Europe, GmbH), with the following thermal cycling conditions: initial 5 min denaturation at 95 °C, followed by 30 amplification cycles of denaturation at 95 °C for 30 s, annealing at 62 °C for 30 s, elongation at 72 °C for 30 s, and a final elongation at 72 °C for 5 min. This amplification product was re-amplified under the same reaction conditions and thermal cycling as above using a T7 promoter – MYCforward primer (5′-TAATACGACTCACTATAGGGAGAGCTCATTTCTGAAGAGGACTTGT-3′). The resulting 252-bp *T7-MYC*-fusion fragment was then PCR amplified using primers MYCreverse and T7 primer (5′-TAATACGACTCACTATAGGGAGA-3′) as described above and purified through band gel extraction. Confirmation of correct PCR products was performed by 2% agarose gel electrophoresis stained with GelRed™. This amplification product was used as template for *in vitro* transcription reactions.

### 2.7. Real-time RT-PCR

To evaluate the expression of the *c-MYC* transcript, Real-time RT-PCR was performed. Real-Time PCR amplification was performed in a Corbett Research Rotor-Gene RG3000 using SYBR GreenER Real-Time PCR Kit (Invitrogen) according to manufacturer's specifications in 50 μl reactions containing 6 μl of cDNA from HCT-116 cells, 1 × SYBR Green SuperMix and 200 nM of primers (STAB Vida)—MYCforward and MYCreverse. The amplification conditions consisted of 50 °C for 2 min hold, 95 °C during 10 min hold, followed by 50 cycles consisting of denaturation at 95 °C for 30 s, annealing at 60 °C for 30 s, extension at 72 °C for 30 s, with a final extension step at 72 °C for 10 min. Data were collected from three independent experiments.

### 2.8. Monitoring RNA synthesis

Standard *in vitro* transcription was performed in 100 μL reaction containing *in vitro* transcription buffer (200 mM Tris-HCl (pH 7.9), 30 mM $MgCl_2$, 50 mM NaCl, 10 mM spermidine), 10 mM of each NTP, 0.6 μg of DNA template, and 30 U of T7 RNA polymerase (Fermentas, Vilnius, Lithuania) according to the manufacturer's protocol. For the real time quantification experiments, 1 nM of the *reporter* Au-nanobeacon (labeled with Cy3) was added to each transcription reaction. When using the *inhibitor* Au-nanobeacon (labeled with FAM), 1 nM was also added to the reaction mixture. All measurements were performed in a PerkinElmer LS45 Fluorescence Spectrometer (USA) using an Ultra-Micro quartz cell (Hëllma, Germany) programmed to incubate the reactions for 120 min at 37 °C while recording the fluorescence intensity of the Au-nanobeacon every 2 min at an excitation wavelength of 490 nm or

530 nm for FAM-labeled or Cy3-labeled Au-nanobeacon, respectively. After the measurements, the enzyme was heat inactivated for 15 min at 75 °C.

All transcription reaction products were also evaluated on a 3% agarose gel electrophoresis with GelRed™ staining. Product quantity determination was performed by pixel intensity/counting using ImageJ™ imaging software as previously described (Luhtala and Parker, 2009).

## 3. Results and discussion

### 3.1. Au-nanobeacon design

We demonstrate the use of Au-nanoparticle based molecular beacon structures (Au-nanobeacons) for real time monitoring of RNA synthesis. First, we designed Au-nanobeacons constituted by AuNPs with an average diameter of 14 nm (see Figure S1 in Supplementary Information) that work both as support structure for the thiolated DNA hairpin structure labeled with Cy3 or FAM and as a quencher to these fluorophores. Much like standard molecular beacons, in the native conformation the hairpin structure is closed and the fluorophore (Cy3 or FAM) and AuNP are brought together, and fluorescence is quenched. In one Au-nanobeacon, the loop in the hairpin structure is complementary to a fragment of the *c-MYC* proto-oncogene mRNA produced by *in vitro* transcription (*reporter*); as transcription occurs, the presence of mRNA target induces the opening of the *reporter*'s structure with concomitant fluorescence intensity increment.

Transcription of a gene into mRNA is highly regulated and can be elegantly switched on and off by blocking the respective promoter. The RNA promoter determines the maximal rate of RNA synthesis and is the site of binding or "initiation" for RNA polymerase. To silence gene transcription, we constructed an *inhibitor* Au-nanobeacon complementary to the promoter region recognized by the T7-RNA polymerase, thus capable of blocking the transcriptional machinery at the specific promoter site and impede transcription. However, the same rationale may be used to target any specific gene sequence of choice, thus blocking a specific gene from being transcribed.

### 3.2. Au-nanobeacon calibration

First, we calibrated the response of the *reporter* Au-nanobeacon to the complementary target using the DNA template that was subsequently used for *in vitro* transcription (see Fig. 2A). A 10-fold increase in fluorescence was detected upon hybridization of the Au-nanobeacon to the complementary target at 37 °C when compared to hybridization to non-related target, showing that the nanobeacon is capable of specific sequence recognition. To ensure that, during transcription, the Au-nanobeacon in solution would not be totally hybridized to the DNA template alone before transcription started, a fixed amount of Au-nanobeacon was added to crescent target concentrations, heated and cooled-down to induce maximum hybridization before transcription.

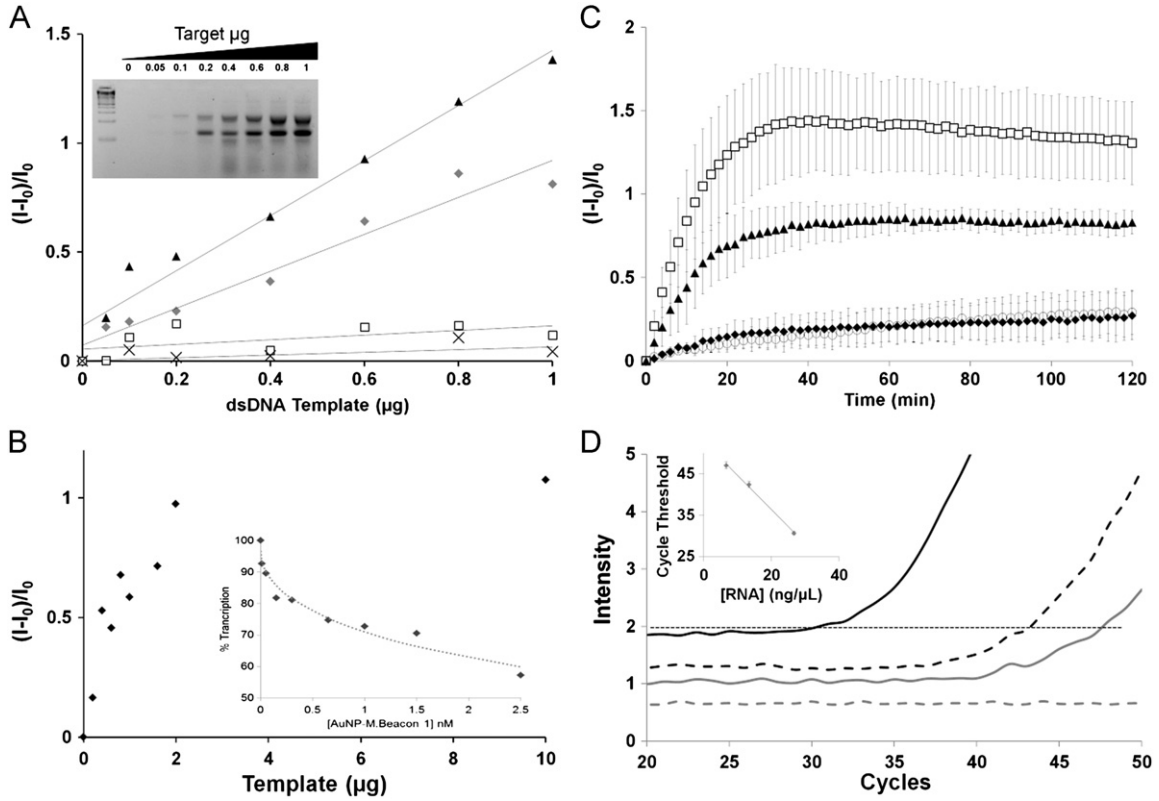


**Fig. 2.** *Au-nanobeacon calibration.* (A) – *Reporter* Au-nanobeacon normalized emission before and after transcription of dsDNA templates that generate complementary (gray diamonds, $y=0.8482x+0.0719$; and black triangles, $y=1.2634x+0.1614$, respectively) and non-complementary (black crosses, $y=0.0618x+0.0018$; and white squares, $y=0.1076x+0.0539$, respectively) RNA products for increasing transcription template. Inset: Agarose gel demonstrating an increase in the intensity of the band corresponding to the transcript for higher template mass. (B) – *Inhibitor* Au-nanobeacon normalized emission in presence of increasing dsDNA template. Inset: Transcription inhibition with increasing amounts of *inhibitor* Au-nanobeacon. (C) – *Reporter* Au-Nanobeacon normalized emission for 120 min at 37 °C in presence of increasing concentrations of total RNA (0 ng/µL – white circles, 6.7 ng/µL – black diamonds, 13.3 ng/µL – black triangles, 26.7 ng/µL – white squares). Error bars represent at least 3 independent assays. (D) – Real-time PCR of the total RNA samples tested with the *reporter* Au-nanobeacon (0 ng/µL – gray dashed line, 6.7 ng/µL – gray full line, 13.3 ng/µL – black dashed line, 26.7 ng/µL – black full line). Inset: Plot of Cycle Threshold *vs.* [total RNA], $y=-0.8721x+54.1$, $R^2=0.9948$. The Threshold Cycle (Ct) represents the cycle number at which the fluorescence produced within a reaction crosses the threshold line (horizontal dotted line at Intensity=2).

Then, the fluorescence intensity of the total system before and after transcription was measured. The fluorescence intensity consistently increases after transcription indicating that, although higher quantities of template correspond to higher fluorescent intensities, there are still hairpin-structures available for specific hybridization to the newly formed transcript. It should be noted that, when compared to traditional molecular beacons, we have more than one hairpin-oligonucleotide per nanoparticle, which results in better signal to background noise, *i.e.* better capability to detect complementary targets that has also been previously reported by others (Cheng et al., 2011). From these calibrating experiments, a working concentration of 0.6 μg of template for the real-time assay was selected. The reporting signal obtained from the *reporter* Au-nanobeacon was further validated by (i) hybridization to total RNA containing complementary target – Fig. 2C; and (ii) real-time quantitative PCR, the *gold standard* for transcript quantification – Fig. 2D. Results corroborate the quantification capability of the *reporter* Au-nanobeacon.

The *inhibitor* Au-nanobeacon presents an average of $4.95 \pm 0.66$ oligomer per AuNP (see Figure S4 in Supplementary Information). We first calibrated the *inhibitor* Au-nanobeacon as described above for the reporter Au-nanobeacon, showing its capability to specifically detect its complementary target sequence inducing a 4.3-fold increase in fluorescence, while not hybridizing to a non-complementary target (Figure S5 in Supplementary Information). In a typical inhibition assay, the dsDNA template (*T7-MYC*) is incubated with increasing concentrations of *inhibitor* Au-nanobeacon and then the transcription reaction is carried out. Following agarose gel electrophoresis, quantification of the amount of mRNA produced in each transcription showed a steady decrease with increasing amount of *inhibitor* Au-nanobeacon, as expected – Fig. 2B. It is clear that the *inhibitor* Au-nanobeacon can effectively compete with the template DNA sequence for RNA polymerase and drastically reduce the level of transcription. This is in clear agreement with previous reports that demonstrate that AuNPs enhance the silencing capability of oligonucleotides, while conveying protection against nucleases (Conde et al., 2010). At the same time it blocks transcription, the *inhibitor* Au-nanobeacon simultaneously signals out the amount of target it is binding to, *i.e.* the fraction of promoters being blocked at any given time.

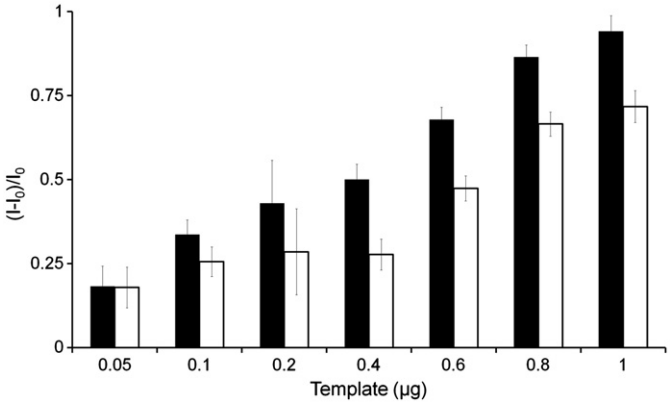


**Fig. 3.** *Au-nanobeacon effect on in vitro transcription. In vitro* transcription in the presence of the reporter Au-nanobeacon (black bars) and in the presence of both reporter (1 nM) and inhibitor (1 nM) Au-nanobeacons (white bars) with increasing amounts of DNA template, measuring the fluorescent intensity of cy3 ($\lambda$=530 nm) for two independent assays ($n$=2). Full bars correspond to average of the assays and the error bars to the respective standard deviation.

### 3.3. Monitoring of RNA synthesis inhibition

We then used the *reporter* and the *inhibitor* Au-nanobeacons simultaneously in the same reaction vial so as to assess transcription and transcription inhibition – Fig. 3. Data show increasing fluorescence output from the *reporter* Au-nanobeacon with increasing concentrations of template that correlates with increasing levels of transcription. The presence of the *inhibitor* Au-nanobeacon (1 nM) can be noted by a decrease in fluorescence from the reporter (1 nM) Au-nanobeacon, showing that it is blocking transcription.

As the concentration of template increases, the level of transcription also increases showing that the same amount of *inhibitor* Au-nanobeacon is blocking a smaller percentage of all the available templates present in the reaction medium. In fact, considering that each AuNP of the *inhibitor* Au-nanobeacon possess an average of five hairpins on its surface, one may assume that all the hairpins per AuNP are in the open conformation if each Au-nanobeacon is blocking five promoters. In this situation the *inhibitor* Au-nanobeacon is saturated and ceases to respond to incremental increases in target concentration, which happens for a concentration of target of about 10 μg ($6.43 \times 10^{-11}$ mol) (see Fig. 2B). Taken this into account and retrieving the fluorescence of the *inhibitor* Au-nanobeacon, it is possible to determine the ratio of promoters being effectively blocked – Table 1. The percentage of promoters being blocked is lower for the higher template concentrations, which correlates to lower inhibition and consequent higher levels of transcription. This way, we demonstrate that this system can effectively quantify the level of RNA synthesis and simultaneously assess the ratio of blocked promoters. To the best of our knowledge, this is the first time a DNA-AuNP conjugate is used to simultaneously silence transcription and quantify the percentage of promoters being effectively blocked.

### 3.4. Real-time assessment of transcription and inhibition – a dual color Au-nanobeacon approach

Based on the previous results, we employed the same approach to follow the *in vitro* transcription in real-time – Fig. 4. We used both Au-nanobeacons in the same RNA synthesis reaction towards a dual-color system for the real time monitoring of both RNA synthesis and level of inhibition. We first measured the fluorescence of the *reporter* Au-nanobeacon for 120 min immediately after the addition of T7 enzyme and NTPs to a previously stabilized solution containing the Au-nanobeacon and template. The reporter Au-nanobeacon signals the continuous synthesis of the complementary mRNA, whilst the production of a non-related transcript induces no changes to the fluorescence intensity. Because of the calibration of the Au-nanobeacon

**Table 1**
*In vitro* transcription inhibition *vs. inhibited* Au-nanobeacon hybridization.

| | | | | | |
|---|---|---|---|---|---|
| Added template ($\text{mol} \times 10^{-12}$) | 1.29 (0.2 μg) | 2.57 (0.4 μg) | 3.86 (0.6 μg) | 5.14 (0.8 μg) | 6.43 (1 μg) |
| Inhibited template ($\text{mol} \times 10^{-12}$) | 0.23 (17.63%) | 0.35 (13.79%) | 0.42 (10.79%) | 0.36 (6.91%) | 0.49 (7.64%) |
| Inhibition of transcription (%) | 96.14 | 90.69 | 66.49 | 62.00 | 56.39 |
| Inhibitor saturation (%) | 45.34 | 70.95 | 83.23 | 71.08 | 98.28 |

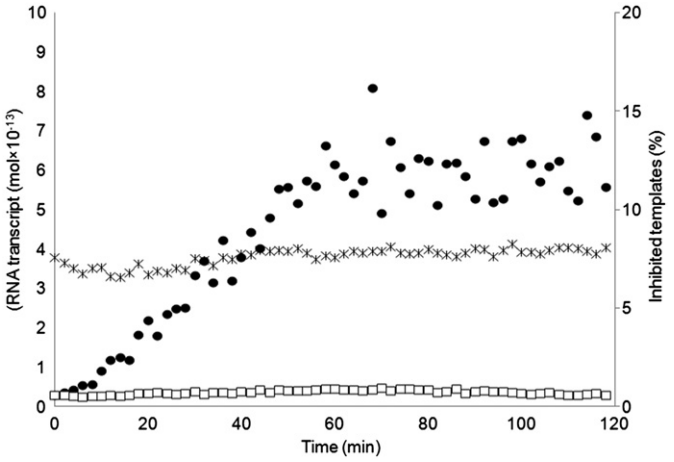


**Fig. 4.** *Real-time in vitro transcription and inhibition using Au-nanobeacons. In vitro* transcription was measured (excitation wavelength of 530 nm, primary axis) in real-time in presence of the *reporter* Au-nanobeacon (black circles) and in simultaneous presence of the *reporter* and *inhibitor* Au-nanobeacons (white squares). The emission of the *inhibitor* Au-nanobeacon was also measured throughout the experience (black stars, secondary axis, and excitation wavelength 490 nm).

previously described it is possible at any time point to correlate directly to the actual amount of RNA being produced (as number of moles or mass). This is extremely relevant if one is to study the regulatory and controlling elements of transcription of a given gene.

We then combined 1 nM of each Au-nanobeacon in one *in vitro* transcription reaction and measured the fluorescent intensity of both fluorophores with excitation at 490 and 530 nm. During the entire reaction time there was no rise in fluorescence associated with production of transcript (*reporter* Au-nanobeacon), showing that the *inhibitor* Au-nanobeacon is effectively blocking the promoter. The *inhibitor*'s emission is constant throughout the entire time lapse, and the percentage of blocked promoters can be easily determined via the procedure described above (7.61%). The level of inhibition of transcription can be easily calculated for each time point. What is more, as can be seen in Figure S7B in Supplementary Information, a normalized intensity curve can be plotted as function of the resulting transcription product retrieved from the agarose gel electrophoresis (see Figure S7A in Supplementary Information).

Real-time monitoring of RNA transcription reactions gave fluorescence plots with an initial lag phase, followed by a first-order increase. The initial lag may be due to assay sensitivity and kinetics of double-helix formation between the Au-nanobeacon and its RNA target. Comparison between the linear phase of the RNA synthesis for the *reporter* Au-nanobeacon (black circles) and *reporter*+*inhibitor* (white squares) demonstrate that we can achieve a 14.1-fold decrease in RNA synthesis after 60 min of transcription (~618 fmol of RNA and ~43.9 fmol of RNA, respectively). These results were confirmed through quantification of transcription via agarose gel electrophoresis (see Figure S8 in Supplementary Information).

## 4. Conclusions

Here, we demonstrate the use of Au-nanobeacons capable of recognizing specific complementary sequences that can be easily synthesized by functionalization of gold nanoparticles with thiolated DNA hairpin oligonucleotides. One of the Au-nanobeacons was designed so as to monitor the synthesis of a specific RNA sequence related to the human proto-oncogene *c-MYC – reporter*; whereas the *inhibitor* was designed to specifically recognize the *c-MYC* sequence downstream of the RNA polymerase T7 promoter, thus blocking transcription in a sequence dependent manner. Because of its beacon conformation, the *inhibitor* is able to simultaneously block the promoter and signal out the number of promoters being effectively blocked. Following Au-nanobeacons calibration, we used them to quantitatively monitor RNA synthesis in real-time and for kinetic quantification of RNA transcript synthesized by a RNA polymerase (~10.3 fmol of RNA per minute of reaction). We also demonstrate that by combining the use of a *reporter* and an *inhibitor* Au-nanobeacon, we were able to create a dual color system capable of quantify transcription and the level of inhibition in a single reaction vial. It is possible to quantify the level of inhibition of the RNA synthesis and relate it to the amount of template being effectively silenced, *i.e.* assessing actual silencing capability. Even though some reports can be found on the use of gold nanoparticles for detection of gene expression, to the best of our knowledge, this is the first time an approach for the simultaneous quantitative monitoring of RNA synthesis and inhibition in real-time is reported. The proposed Au-nanobeacon biosensor allows for fast, accurate and sensitive RNA transcript expression profiling. A unique feature of this sensor, compared to conventional measurements of polymerase activities using intercalating dyes, is that the probes do not generate a signal from unrelated nucleic acids and polymerase activities can be distinguished from promoter-specific RNA polymerization. The simplicity and speed of the sensor are also great advantages.

This new Au-nanobeacon sensor allows extending quantification of gene expression to real-time assessment of transcription and inhibition, thus providing means to evaluate the potential of a given sequence to effectively silence a target gene. Also, because the AuNPs confer resistance to nuclease degradation, these sensors may be used to follow gene silencing *in vivo*, thus providing additional information to assist modeling of actual gene therapy protocols. Nevertheless, before *in vivo* utilization, exhaustive studies need to be conducted in situations of increasing complexity, *e.g.* complex reaction mixtures, cell extracts and cell lineages.

## Acknowledgments

This work was supported by Fundação para a Ciência e Tecnologia [CIGMH, REQUIMTE, PTDC/QUI-QUI/112597/2009, SFRH/BD/43320/2008 to J.R., SFRH/BD/62957/2009 to J.C.]; Nanotruck-Action from NanoSciEra+; ARAID to J.M.F.

## Appendix A. Supporting information

Supplementary data associated with this article can be found in the online version at http://dx.doi.org/10.1016/j.bios.2012.04.006.

## References

Agbasi-Porter, C., Ryman-Rasmussen, J., Franzen, S., et al., 2006. Bioconjugate Chemistry 17, 1178–1183.
Agrawal, S., 1996. Trends in Biotechnology 14, 376–387.
Baptista, P., 2009. Current Cancer Therapy Reviews 5, 80–88.
Baptista, P., Pereira, E., Eaton, P., et al., 2008. Analytical and Bioanalytical Chemistry 391, 943–950.
Bor, Y.C., Swartz, J., Li, Y., Coyle, et al., 2006. Nature Protocols.
Cheng, Y., Stakenborg, T., Van Dorpe, P., et al., 2011. Analytical Chemistry 83, 1307–1314.
Conde, J., de la Fuente, J.M., Baptista, P.V., 2010. Nanotechnology 21, 1–6.

Dubertret, B., Calame, M., Libchaber, A.J., 2001. Nature Biotechnology 19, 365–370.
Fichou, Y., Ferec, C., 2006. Trends in Biotechnology 24, 563–570.
Freeman, W.M., Walker, S.J., Vrana, K.E., 1999. Biotechniques 26, 112–115.
Lakowicz, J.R., 2006. Plasmonics 1, 5–33.
Lee, P.C., Meisel, D., 1982. The Journal of Physical Chemistry 86, 3391–3395.
Li, J.J., Fang, X., Schuster, S.M., 2000a. Angewandte Chemie-International Edition 39, 1049–1052.
Li, J.J., Geyer, R., Tan, W., 2000b. Nucleic Acids Research 28, 1–6.
Liu, J., Feldman, P., Chung, T.C., 2002. Analytical Biochemistry 300, 40–45.
Luhtala, N., Parker, R., 2009. Nucleic Acids Research 37, 5529–5536.
Marras, S.A., Gold, B., Kramer, F.R., et al., 2004. Nucleic Acids Research 32, 1–6.
Paciotti, G.F., Myer, L., Weinreich, D., et al., 2004. Drug Delivery 11, 169–183.
Quarta, A., Di Corato, R., Manna, L., et al., 2007. IEEE Transactions on Nano-Bioscience 6, 298–308.
Rayburn, E.R., Zhang, R., 2008. Drug Discovery Today 13, 513–521.
Rosi, N.L., Giljohann, D.A., Thaxton, C.S., et al., 2006. Science (New York, NY) 312, 1027–1030.
Saha, K., Agasti, S.S., Kim, C., et al., 2012. Chemical Reviews. Article ASAP.
Schena, M., Shalon, D., Davis, R.W., et al., 1995. Science (New York, NY) 270, 467–470.
Seferos, D.S., Giljohan, D.A., Hill, H.D., Prigodich, et al., 2007. Journal of the American Chemical Society 129, 15477–15479.
Song, S., Liang, Z., Zhang, J., et al., 2009. Angewandte Chemie-International Edition 48, 8670–8674.
Tamm, I., Dorken, B., Hartmann, G., 2001. Lancet 358, 489–497.
Tan, W., Wang, K., Drake, T.J., 2004. Current Opinion in Chemical Biology 8, 547–553.
Toub, N., Malvy, C., Fattal, E., Couvreur, P., 2006. Biomedicine and Pharmacotherapy—Biomedecine and Pharmacotherapie 60, 607–620.
Tyagi, S., Kramer, F.R., 1996. Nature Biotechnology 14, 303–308.
Waltz, T.L., Marras, S., Rochford, G., et al., 2005. Journal of Clinical Microbiology 43, 254–258.
Weis, J.H., Tan, S.S., Martin, B.K., et al., 1992. Trends in Genetics 8, 263–264.